Colloids and Surfaces A: Physicochem. Eng. Aspects 480 (2015) 253–259

Contents lists available at ScienceDirect

Colloids and Surfaces A: Physicochemical and Engineering Aspects

journal homepage: www.elsevier.com/locate/colsurfa

Thermal and phase behavior of didodecyldimethylammonium bromide aqueous dispersions

Eloi Feitosa[a,*], Renata D. Adati[a], Fernanda R. Alves[b]

[a] Department of Physics, São Paulo State University, São Jose do Rio Preto, SP, Brazil
[b] Instituto de Química de São Carlos, Universidade de São Paulo, São Paulo, SP, Brazil

HIGHLIGHTS

- On increasing DDAB concentration, the following phase sequence appears: monomer, vesicle, lamellae.
- DDAB unilamellar vesicles are formed in water only in a very narrow concentration range.
- DDAB multilamellar vesicles co-exist with unilamellar vesicles in this concentration range.
- Phase separation occurs in DDAB/water, with lamellae on top and vesicles on bottom.
- The reverse melting temperature of DDAB/water is around 9.5 °C.

GRAPHICAL ABSTRACT

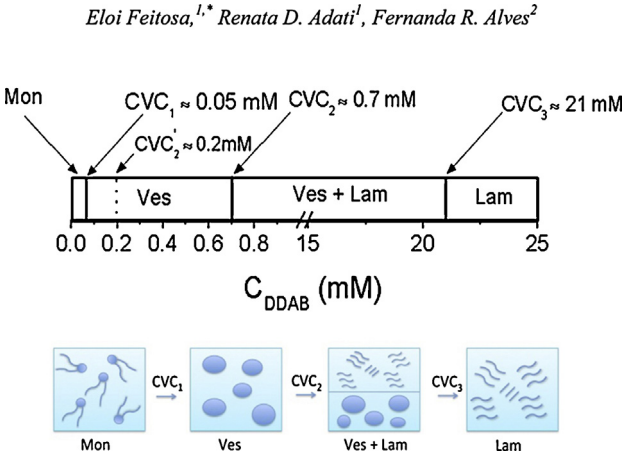

ARTICLE INFO

Article history:
Received 22 June 2014
Received in revised form 18 January 2015
Accepted 24 January 2015
Available online 9 February 2015

Keywords:
Cationic vesicles
DDAB
Differential scanning calorimetry
Dynamic light scattering
Gel-liquid crystalline transitions
Zeta potentials

ABSTRACT

This work aims to delineate the single isotropic vesicle phase (Ves) in the binary didodecyldimethylammonium bromide (DDAB)/water system, limited by the critical vesicle concentrations, $CVC_1 \approx 0.05$ mM (2.3×10^{-3} wt%) and $CVC_2 \approx 0.7$ mM (3.1×10^{-2} wt%), as the onset of unilamellar vesicle formation and of two-phase separation into Ves + Lam (lamellar) phases, respectively. Isothermal titration calorimetry (ITC), turbidity, and crossed polaroids observations indicate that below CVC_1 the dispersion is dominated by free monomers or micelles, but rich in uni- and multilamellar vesicles between CVC_1 and CVC_2, with $CVC_2 = 0.21$ mM (9.5×10^{-3} wt%) being the onset of multilamellar vesicle formation. Above CVC_2, the volume of the Lam phase increases, while the volume for the Ves phase decreases to vanish around $CVC_3 \approx 21$ mM (0.95 wt%). Differential scanning calorimetry (DSC) data show that the gel-to-liquid crystalline transition at $T_m \approx 16$ °C is highly cooperative ($\Delta T_{1/2} \approx 0.3$ °C), and the melting enthalpy (ΔH_m) increases with DDAB concentration. Because of the remarkably slow liquid crystalline-to-gel kinetics, a cooling transition around $T_m' \approx 9.5$ °C is reported here for the first time, we ascribe to the liquid crystalline-to-gel transition (thermal hysteresis $\Delta T_m \approx 6.5$ °C). Vesicle and lamellar structure formation

* Corresponding author at: Department of Physics, São Paulo State University, Rua Cristovao Colombo, 2265, 15.054-000, Sao Jose do Rio Preto, SP, Brazil.
E-mail address: eloi@ibilce.unesp.br (E. Feitosa).

http://dx.doi.org/10.1016/j.colsurfa.2015.01.086
0927-7757/

is supported also by hydrodynamic diameter (D_H) data, being 100–140 and 800–1200 nm, respectively, at 25 °C. The zeta potential (ζ) increases with DDAB concentration but does not change much with temperature, indicating no pronounced structural change when temperature varies around T_m.

1. Introduction

Synthetic double-chain surfactant vesicles, such as those formed from the double-chain cationic didodecyldimethylammonium bromide (DDAB) in aqueous dispersion [1], is attracting increasing interest in fields as nanomedicine because of their strong interaction with nucleic acids, such as DNA or RNA, and formation of lipoplexes in presence of nanoparticles for transfection purposes [2]. It has been reported that above the critical vesicle concentration (CVC) and above its gel-to-liquid crystalline [3], or hydrated crystalline-to-liquid crystalline [4], temperature ($T_m \approx 16$ °C), DDAB self-assembles in water as vesicles [3,5,6]. Even though the phase behavior of DDAB/water have already been reported [7–10], the effect of DDAB concentration on the bilayer structural organization, however, has been only poorly explored. Besides structural size, T_m and CVC play important role on the characterization of this system. Unlike T_m, the CVC of DDAB in aqueous solution is not uniquely determined. The CVC value depend on the technique used to determine it, while to our knowledge T_m of DDAB has been determined only by DSC [3–6]. Then, what is the physical meaning of CVC values of DDAB? To our knowledge, the actual DDAB concentration range in which single vesicles can be prepared is still undetermined. It has been reported that the structure of DDAB vesicles becomes increasingly complex when the surfactant concentration is augmented, due the formation of multilamellar structures [6–8]. As demonstrated here in detail, DDAB unilamellar vesicle is the preferable structure only within a very narrow range of concentration (0.05–0.7 mM), hardly investigated so far.

The phase behavior for more extended DDAB concentrations have been reported [9–12] and correlated with CVC or CMC values [9] owing to vesicle or micelle formation as well as with structure curvature [9] and osmotic pressure [12]. Dubois and Zemb [12] reported a complete X-T binary phase diagram indicating an isotropic region roughly below 4 mM (ca. 0.2 wt%) DDAB, while the two-phase region (vesicle plus extended lamellae) ranges up to ca. 30 wt% surfactant. These authors sustained that the formation of multilamellae was induced by osmotic pressure effects, causing swelling of the surfactant bilayers thus favoring more complex structures [12].

Despite these previous studies, important properties of DDAB vesicles, the main object of our study, still remain unresolved. For example, both the CVC and vesicle size seem to depend on the method used to prepare and investigate the dispersion (Table S1 and S2, Supporting Materials). This spread in results is probably related to the slow liquid-crystalline-to-gel kinetics of DDAB [3,13], combined with experimental problems related with the system phase separation even at very low DDAB concentration [9], as well as surfactant purity (we used non treated DDAB as supplied by the manufacturer). In addition, the influence of the slow kinetics on the self-assembly in the gel state has not been properly clarified [3,13]. Due to experimental challenges related with the low range of vesicle concentration of interest, as well as low light scattering and slow kinetics, the high sensitivity differential scanning calorimetry (DSC) and isothermal titration calorimetry (ITC) offer unique opportunities for investigation of these effects. Herein, we therefore combined DSC and ITC studies with turbidity, crossed polaroid, dynamic light scattering (DLS), and dynamic electrophoretic light scattering (DELS), in order to investigate the phase behavior of dilute DDAB/water dispersions, together with their thermal properties, with particular focus on the slow kinetic behavior of the vesicle system.

2. Materials and methods

2.1. Material

DDAB (MW 462.65 g/mol, purity 98%) was obtained from Sigma-Aldrich (St. Louis, USA), and used without further purification. Milli-Q® ultrapure water with a resistivity 18.2 MΩ cm at 25 °C was used throughout. All samples were prepared at 25 °C by adding water to the DDAB powder. The mixtures were gently stirred for at least 24 h prior to DSC or scattering measurements. The samples were also equilibrated at room temperature (25 °C) for several months for the phase diagram construction.

2.2. Characterization

CVC_1 and CVC_2 were determined by DSC, ITC, and turbidity measurements. For this purpose, 2.5 mL of DDAB/water samples were placed in a 1.0 cm path-length squared quartz cell, and turbidity measurements performed at 250 nm and 25 °C as a function of DDAB concentration, using a Cary 300 Bio UV–vis spectrophotometer (Varian, Mulgrave, Australia).

A light scattering setup (Brookhaven Instruments Corporation, Holtsville, USA), equipped with an adjustable 15 mW maximum power He-Ne laser (wavelength 633 nm), was used to obtain the hydrodynamic diameter (D_H) of DDAB vesicles at selected surfactant concentrations and temperatures, at a scattering angle $\theta = 90^o$. From the translational diffusion coefficients, the hydrodynamic diameter D_H was obtained through the Stokes–Einstein relation.

The zeta potential (ζ) of the DDAB (Ves and/or Lam) aggregates were measured, at selected surfactant concentrations and temperatures, using a dynamic electrophoretic light scattering equipment (ZetaPals, Brookhaven Corporation, Holtsville, USA) equipped with a 632.8 nm He-Ne laser operating at 35 mW. The hydrodynamic diameter D_H of the vesicles and complexes was also measured using this equipment.

DSC measurements were performed on a VP-DSC microcalorimeter (MicroCal Inc., Northampton, MA, USA) at an external pressure of ca. 180 kPa. The twin cells (volume 0.517 mL) were filled with sample and reference (water). Three or more consecutive DSC heating scans from 1 to 45 °C were performed at a scanning rate of 20 °C/h (if not otherwise indicated) and varying pre-scan times as indicated in the text. All scans were normalized after subtracting the reference data (water sample). Details on the equipment setup are reported elsewhere [3].

ITC data were collected on a high precision microcalorimeter VP-ITC (MicroCal LLC, Northampton, MA, USA). The enthalpy changes (ΔH_{obs}) were obtained by injecting DDAB (at 1.0 or 10 mM) into the 1.4 mL reaction cell containing water at 25 °C. The experiments were performed by one injection of 2 μL, followed by 40 injections of 7 μL with a 240 s interval between each injection. The DDAB dispersion in the cell was stirred at 300 rpm. The enthalpy changes per mole of DDAB evolved after each injection was obtained from

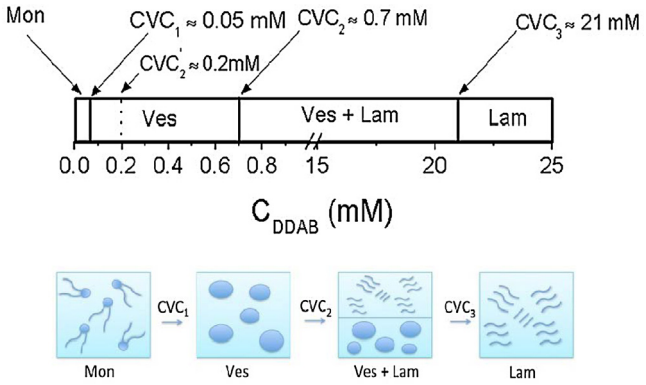

Fig. 1. Top: Phase map (25 °C) of DDAB/water, showing the phase sequence: Monomer (Mon), Vesicle (Ves), Ves + Lamellae (Lam), and Lam. CVC values: $CVC_1 \approx 0.05$ mM, $CVC_2' \approx 0.21$ mM, $CVC_2 \approx 0.7$ mM and $CVC_3 \approx 21$ mM. Bottom: Schematic representation of structures dominated in these regions.

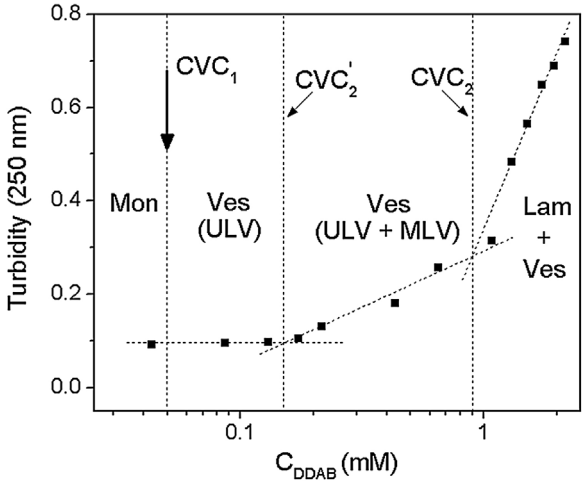

Fig. 2. Effect of DDAB concentration on turbidity of DDAB/water measured at 25 °C.

integration of the endothermic peaks and displayed as a function of the final DDAB concentration.

3. Results and discussion

3.1. DDAB/water phase map

Upon addition of DDAB to water at 25 °C, our data herein suggest the following phase sequence (Fig. 1): monomer (Mon) or micelle (Mic), vesicle (Ves), Ves + Lam (lamellar), and Lam, in agreement with previous observations [10–12]. Accordingly, $CVC_1 \approx 0.05$ mM (2.3×10^{-3} wt%) and $CVC_2 \approx 0.7$ mM (3.1×10^{-2} wt%) as the lower and higher borders of the Ves phase, respectively, and the formation of a single Lam phase beyond $CVC_3 \approx 21$ mM (0.95 wt%). A $CVC_2' \approx 0.21$ mM (9.5×10^{-3} wt%) found by ITC (see Fig. 3b) may be related to the onset of multilamellar structure formation which co-exists with the vesicles in the Ves phase.

The phase behavior (Fig. 1) was obtained from DDAB/water samples equilibrated for several months, followed by inspection through crossed polarizers, DSC, ITC, and scattering analysis. DSC and ITC data revealed the CVC_1 and CVC_2 values, while crossed polarizers helped estimate the CVC_2 and CVC_3 values, respectively, for the lower and higher borders of the (Ves + Lam) two-phase

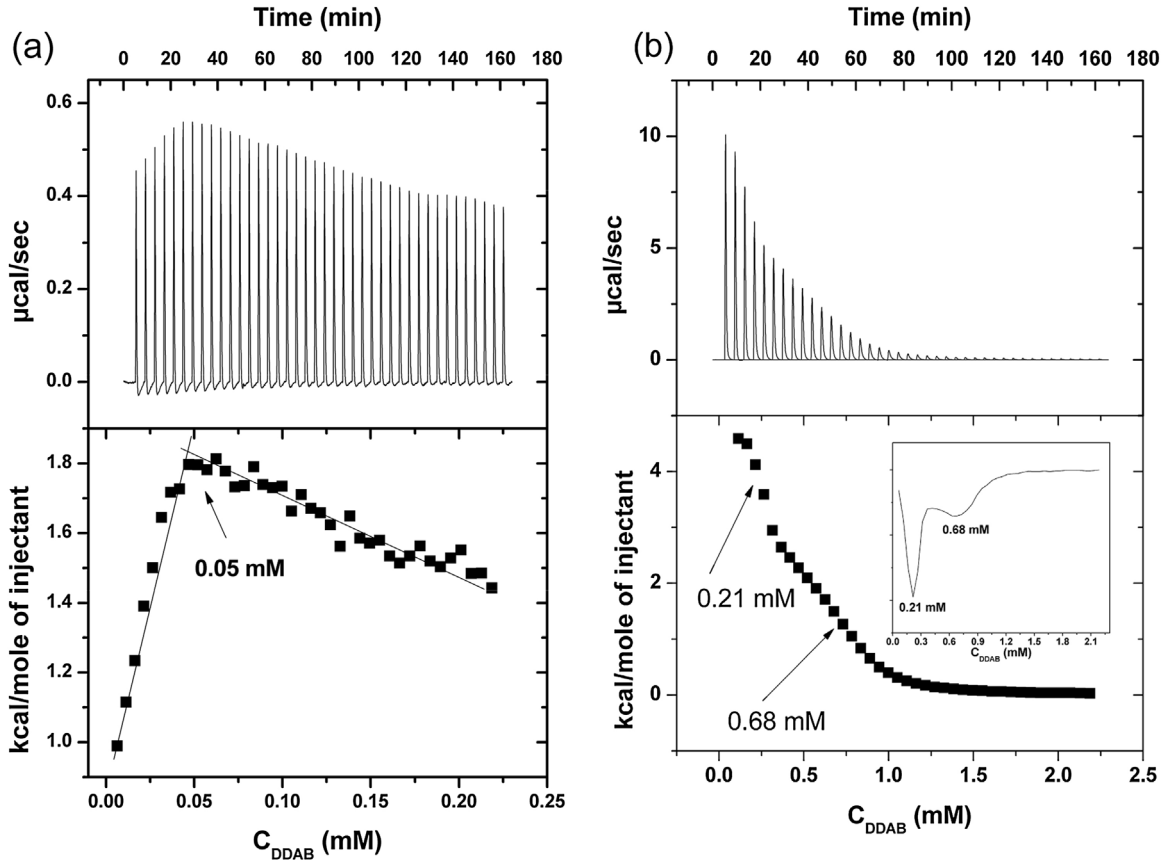

Fig. 3. Titration curves for DDAB 1.0 mM (a) and 10 mM (b) at 25 °C. Effect of DDAB concentration on the observed enthalpy change per mole (ΔH_{obs}) related to each injection for DDAB 1.0 mM (a, bottom) and 10 mM (b, bottom). Arrows indicate the CVC_1, CVC_2' and CVC_2 values.

region. CVC_2' was determined by ITC and turbidity (Table S2, Supporting Materials).

3.2. Turbidity

Fig. 2 displays the effect of DDAB concentration on the turbidity (optical density) of DDAB in water at 25 °C. These data mainly indicate: (i) below CVC_2', turbidity is very low, suggesting the presence of single micelles or vesicles; (ii) between CVC_2' and CVC_2, turbidity increases, suggesting the presence of larger structures (MLV) that co-exist with the ULVs; (iii) above CVC_2 turbidity raises steeply, indicating the presence of even larger multilamellar structures. The intercepts of the fitting curves to the experimental turbidity data give $CVC_2' \approx 0.15$ mM (6.8×10^{-3} wt%) and $CVC_2 \approx 0.9$ mM (4.1×10^{-2} wt%).

3.3. Isothermal titration calorimetry (ITC)

Fig. 3a (top) and b (top) show representative endothermic heat flow as a function of time after micro-injections of DDAB dispersions at 1 and 10 mM, respectively, into the reaction cell containing water, at 25 °C. When 1 mM DDAB is added into the cell, the observed enthalpy changes (ΔH_{obs}), initially increases and then decreases with increase in DDAB concentration (Fig. 3a, bottom). We ascribe the curve maximum to $CVC_1 \approx 0.05$ mM (2.3×10^{-3} wt%), obtained from the intercept of the fitting curves (Fig. 3a bottom). Below CVC_1, the increase in ΔH_{obs} results from the vesicle dissociation into monomers, while above CVC_1, ΔH_{obs} decreases due to vesicle dilution.

Upon injection of 10 mM DDAB, the curve displays two transitions around $CVC_2' \approx 0.2$ and $CVC_2 \approx 0.7$ mM DDAB (Fig. 3b, bottom), as obtained from the derivative of the enthalpy curve (insert in Fig. 3b). This CVC_2 value corroborates the one obtained by crossed polaroids, DSC and turbidity (Fig. 2 and Table S2). CVC_2' might indicate the onset of MLV formation, which co-exists with ULV prior phase separation. Below CVC_2', ΔH_{obs} change is due to vesicle and lamellae dissociation and vesicle dilution (at 10 mM DDAB is a Ves + Lam dispersion); between CVC_2' and CVC_2, ΔH_{obs} arises from vesicle dilution and lamellae dissociation; while above CVC_2 it is due to vesicle and lamellae dilution, since after CVC_2 ΔH_{obs} is significantly smaller and attain the same level (Fig. 3b, bottom).

3.4. Hydrodynamic size

DDAB dispersions display a single broad or a two-mode size distribution function (Fig. 4a), typical for polydisperse samples [14], Fig. 4b shows the effect of temperature on the mean apparent hydrodynamic diameter (D_H) of DDAB vesicles and lamellae at 1 mM. Accordingly, below T_m, $D_H \approx 100$ and 500–600 nm, respectively for the vesicles and lamellae, while above T_m, these aggregates are bigger, $D_H \approx 100$–300 nm and 600–850 nm, respectively (Fig. 4b). These values are in line with previous findings using cryo-TEM images of single and double layered structures in the range of 50–500 nm for 2.5 mM DDAB [7]. According to Fig. 4c, the dispersion is highly polydisperse, and the Lam structures (500–1500 nm) are much bigger than the Ves structures (150–170 nm). These results support our ITC findings on the formation of large multilamellar structures above $CVC_2' \approx 0.2$ mM (Fig. 3b).

3.5. Zeta potential

According to Fig. 5a, ζ increases linearly with DDAB concentration, but at a smaller rate above $CVC_2 \approx 0.6$ mM (Fig. 5a), while ζ

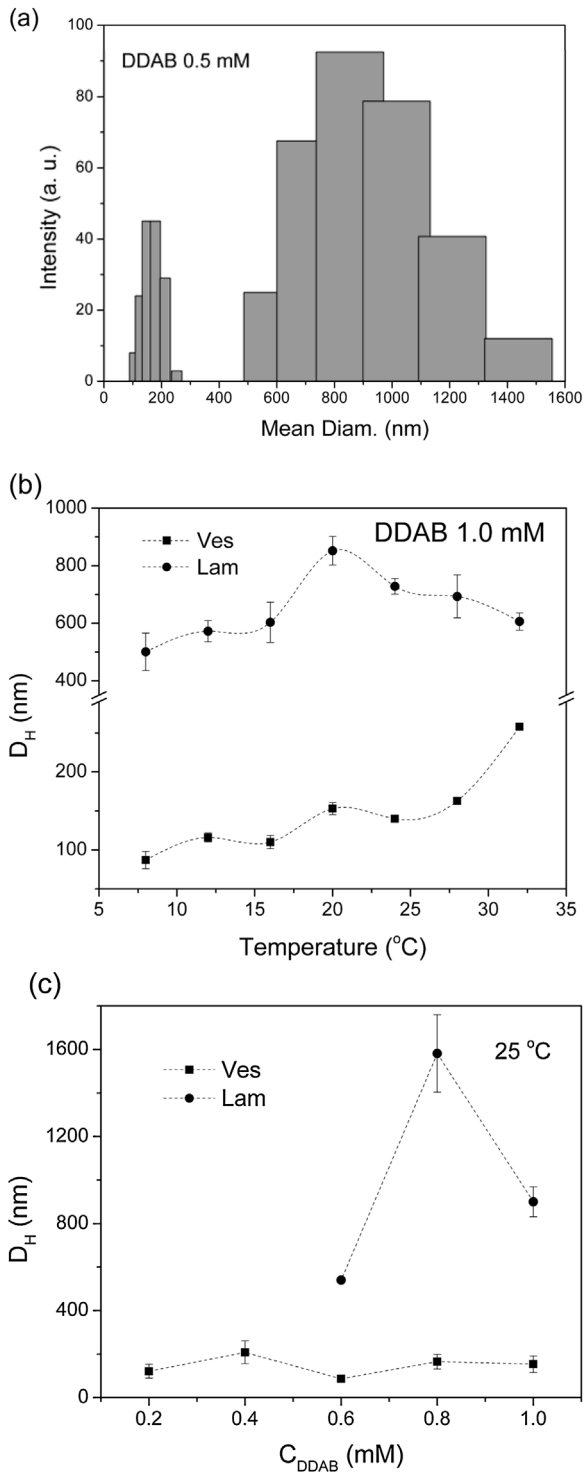

Fig. 4. (a) Size distribution of a 0.5 mM DDAB dispersion at 25 °C. Effects of temperature (b) and DDAB concentration (c) on D_H of DDAB Ves and Lam structures, at 25 °C.

is roughly constant below $T_m \approx 16$ °C and decreases slightly above this temperature (Fig. 5b). Overall, there are only mild changes in ζ as the temperature or surfactant concentration goes past T_m or CVC_2, indicating that there is no striking structural changes in the aggregate structure, in good accord with D_H data (Fig. 4). In line with the higher packing density of Lam compared to Ves, the increase in ζ results from the formation of lamellar aggregates with increasing DDAB concentration. The increase in ζ with increasing DDAB

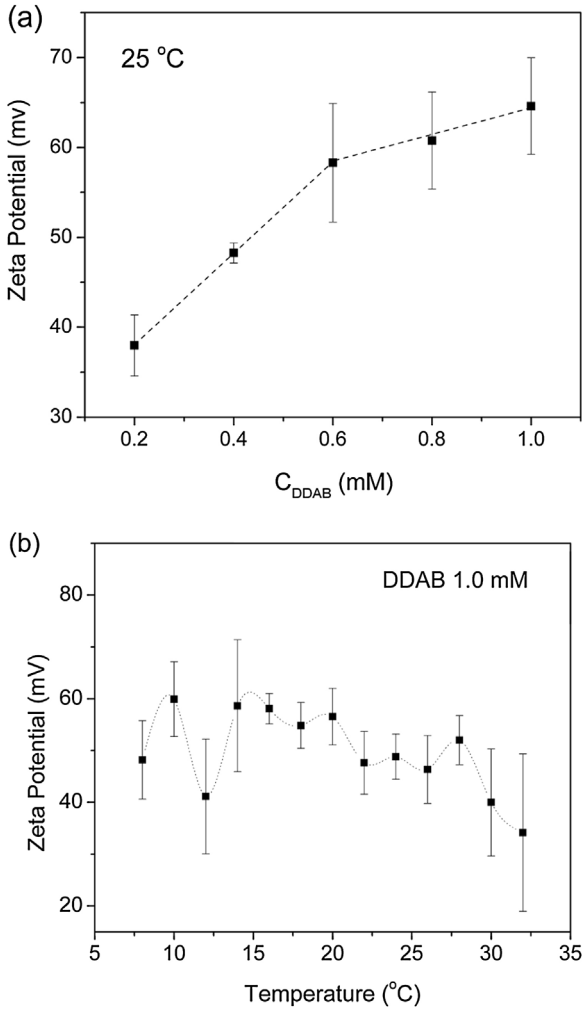

Fig. 5. Effects of [DDAB] at 25 °C (a) and temperature at 1.0 mM DDAB (b) on ζ of DDAB (Ves and Lam) structures.

concentration may be due to change in concentration rather than change in the structure size.

3.6. Thermal behavior of DDAB in water

The existence of bilayer structures in the Ves phase was confirmed by DSC thermograms (Fig. 6), which display a sharp gel-to-liquid crystalline [3], or hydrated crystalline to the liquid crystalline [4], transition at $T_m \approx 16$ °C. The upper border of the Ves phase (at $CVC_2 \approx 0.7$ mM) is the onset of the phase separation, with formation of a Lam top phase [9,11,12]. In the two-phase region of the phase diagram (Fig. 1), the volume of the Lam phase expands, while the Ves phase shrinks, upon increasing DDAB concentration until $CVC_3 \approx 21$ mM, when the sample becomes a single birefringent Lam phase above T_m and milky below T_m. Samples from the Lam phase display also a single endotherm at $T_m \approx 16$ °C, indicating that T_m is characteristic of DDAB bilayers in both the Ves and the Lam structures.

Having determined the borders (CVC_1, CVC_2, and CVC_3) of DDAB/water phase map at 25 °C (Fig. 1), we then investigated in detail the thermal behavior of DDAB bilayers. Unlike CVC (see Table S1 and S2 and Refs. [16–21]), T_m (Table S3) is well-defined for DDAB in water ($T_m \approx 16$ °C) and highly cooperative (peak width $\Delta T_{1/2} < 0.5$ °C) [2,5,13]. To the best of our knowledge the reverse liquid crystalline-to-gel transition temperature (T_m'), has not been reported for DDAB so far because of its exceedingly slow kinetics

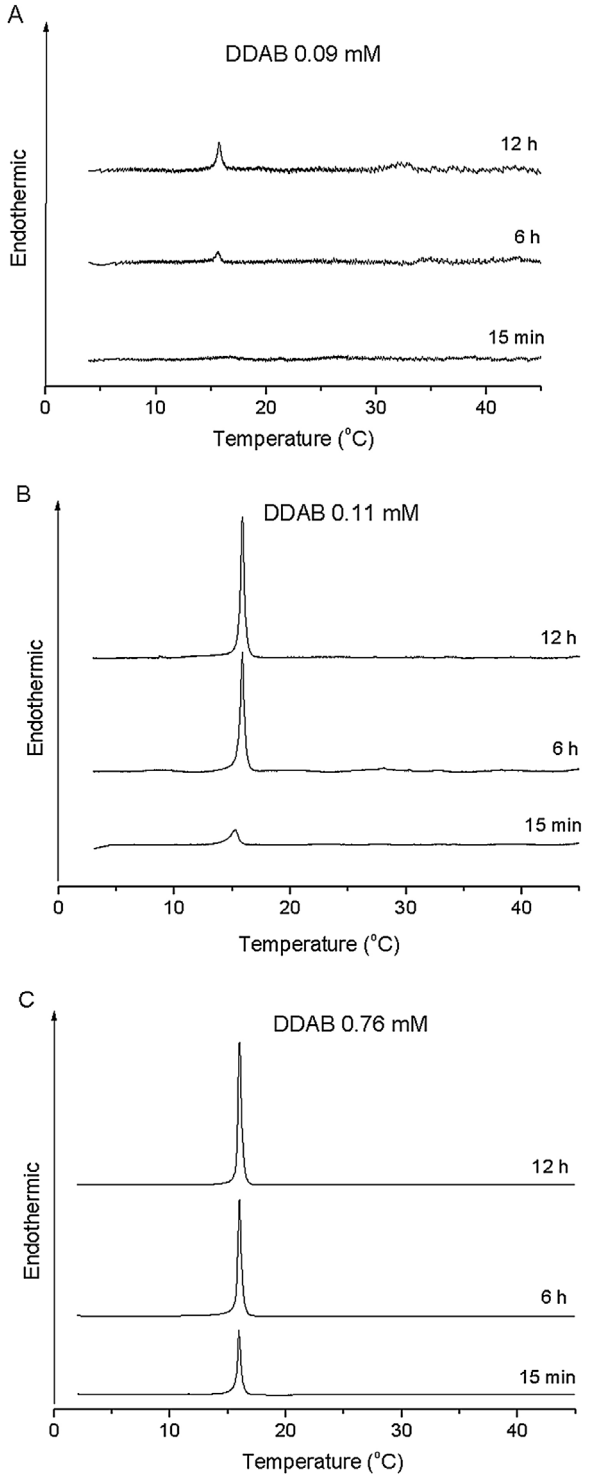

Fig. 6. DSC heating thermograms for DDAB/water at 0.09 (a), 0.11 (b) and 0.76 mM (c), obtained at pre-scan time 15 min, 6 h, and 12 h, respectively.

[3,13]. We investigated the effect of the equilibrium (pre-scan) time on the heating DSC thermogram of DDAB dispersions, aiming to detect the characteristic thermogram with a single endotherm at T_m [3–5,13].

Fig. 6 shows DSC thermograms of DDAB at 0.09, 0.11 and 0.76 mM, in the single Ves phase, obtained using pre-scan times of 0.25, 6 and 12 h. According to Table S4 (Supporting Materials), $T_m \approx 16$ °C and $\Delta T_{1/2} \approx 0.3$ °C do not depend on DDAB concentration or on the structural organization of the surfactants as uni- or

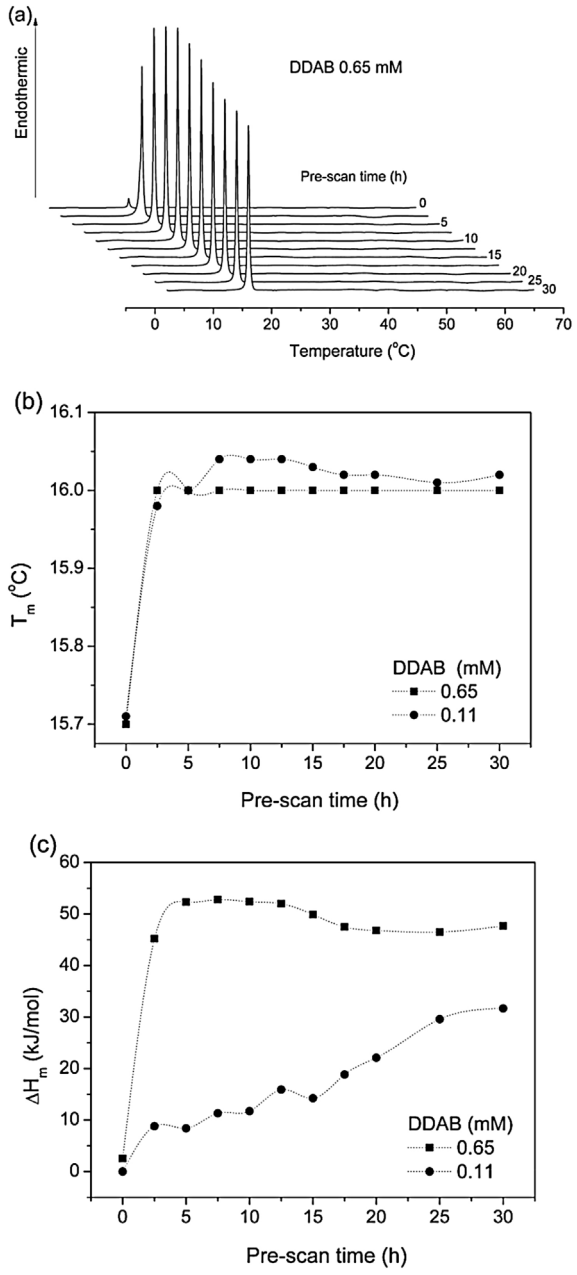

Fig. 7. (a) DSC heating thermograms for DDAB at 0.65 mM, at increasing pre-scan time up to 30 h. The offset between successive traces equals 2.0 °C. Effect of pre-scan time on T_m (b) and ΔH_m (c) for DDAB at 0.11 and 0.65 mM.

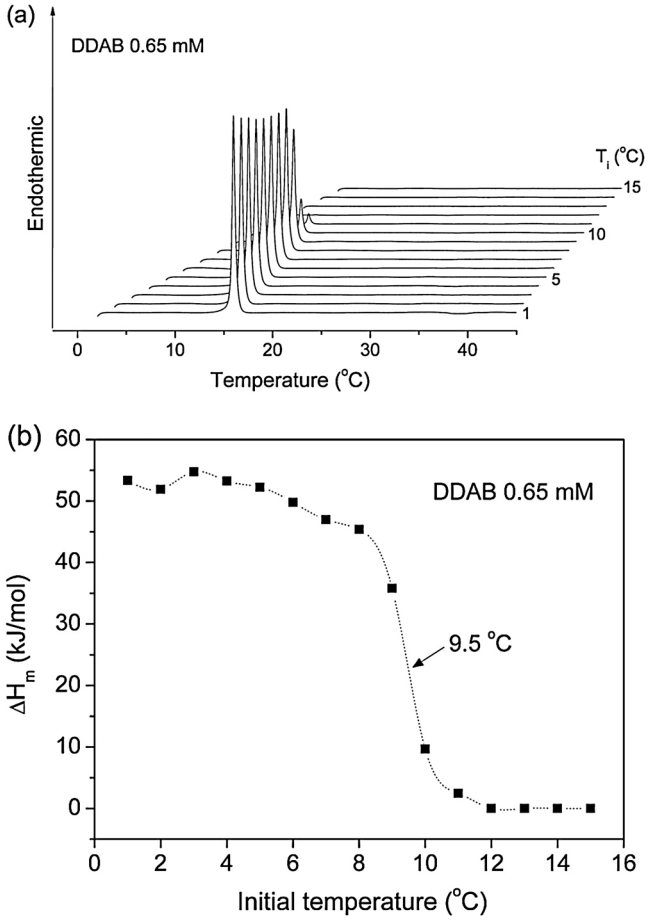

Fig. 8. (a) DSC thermograms for DDAB 0.65 mM, for initial heating temperatures varying from 15 to 1 °C at steps of 1 °C. (b) Effect of T_i on ΔH_m. Arrow points to the T_m' value.

multilamellar structures. Furthermore, for a given pre-scan time, the endotherm enthalpy (ΔH_m) increases with DDAB concentration, indicating that the assembly kinetics increases with increasing DDAB concentration (Table S4). The increase in enthalpy with equilibrium time reflects the slower cooling T_m' -transition relative to the T_m-transition, as reported [3–5,13].

Fig. 7a shows representative heating thermograms for DDAB at 0.11 and 0.65 mM for varying the pre-scan time up to 30 h at steps of 1 °C. Accordingly, T_m varies only in the range 15.7–16.0 °C (Fig. 7b), while ΔH_m increases steeply with pre-scan time to a maximum value of $\Delta H_m \approx 52$ kJ/mol, and stabilizes in $\Delta H_m \approx 47$ kJ/mol for DDAB 0.65 mM (Fig. 7c). The decrease in enthalpy with equilibrium time may be due to a partial crystallization of the surfactants exposed for long time to a temperature below the Krafft point [3].

For the lower concentrated 0.11 mM, ΔH_m increases monotonically to 30 kJ/mol, again indicating that both concentration and equilibration time determine the equilibrium condition (Fig. 7c). Alternatively, at 0.11 mM DDAB, a longer equilibrium time may be required. In comparison, Marques et al. [6] obtained a lower estimate of $\Delta H_m = 25$ kJ/mol, using a shorter equilibrium time, potentially causing the heating process to start at a non-equilibrium condition, while Goto et al. [4] reported a higher enthalpy value, $\Delta H_m = 76.9$ kJ/mol, but at a considerably higher DDAB concentration (5 mM).

As the cooling transition is much slower than the heating transition, ΔH_m is expected to increase with increasing pre-scan time until equilibrium is attained (Fig. 7c). To approach the equilibrium condition, ΔH_m should be obtained after a long enough equilibrium time in the gel state. After 5 h, equilibrium is attained for DDAB at 0.65 mM, giving $\Delta H_m \approx 52$ kJ/mol, but an even longer time (>30 h) is necessary for the lower concentrated DDAB 0.11 mM (Fig. 7c). These data indicate that the equilibrium time is inversely proportional to DDAB concentration, and ΔH_m (but not T_m) depends both on DDAB concentration and equilibrium time.

3.7. Liquid crystalline-to-gel transition

To our knowledge, the temperature of the liquid crystalline-to-gel reverse transition (T_m') for DDAB in water has not been reported so far. On heating, the endotherm appears only if the

sample is (completely or partially) in the gel state at the initial heating temperature (T_i). Firstly, we attempted to detect T_m' by running a cooling DSC experiment, from 65 to 1 °C, at the lowest scan rate of 0.1 °C/h allowed by the instrument, but no exotherm was observed (not shown). In an alternative approach, a series of heating experiments was performed starting at $T_i < T_m$ and ending at $T_f = 45$ °C. In such experiments, it was expected that the endotherm would appear, completely or partially, only when T_i were around T_m'. The thermograms (Fig. 8a) indicate that the melting endotherm was detected only when $T_i \leq 11$ °C and the plot of ΔH_m vs. T_i (Fig. 8b) shows a steep transition around $T_m' \approx 9.5$°C, the liquid crystalline-to-gel temperature. When $T_i < 5$ °C, ΔH_m is constant at $\Delta H_m \approx 52$ kJ/mol, the maximum (stabilizing) heating enthalpy of DDAB. For higher T_i values, the transition is only partial, and does not exist at all above 11 °C. This reverse transition is broader than the corresponding T_m transition, and there is a hysteresis $\Delta T_m = T_m - T_m' \approx 6.5$°C, close to the 5 °C hysteresis reported for the homologue C_{18} (DODAB), which displays both the heating and cooling peaks around 45 and 40 °C, respectively [15].

4. Conclusions

We reported here on the thermal properties of DDAB aqueous dispersions, highlighting the Ves composition, displaying $CVC_1 \approx 0.05$ mM and $CVC_2 \approx 0.7$ mM as the border lines, characteristic of the onset of vesicle formation and Ves/Lam phase separation, respectively. ITC and turbidity revealed an intermediate $CVC_2' \approx 0.2$ mM, as the onset multilamellar structure formation. Above $CVC_3 \approx 21$ mM the dispersion was dominated by lamellar structures.

As the liquid crystalline-to-gel transition of DDAB at $T_m' \approx 9.5$°C (determined here) is much slower than its reverse at $T_m \approx 16$ °C, the cooling exotherm could not be detected by DSC. T_m' was then identified by varying the initial heating temperature (T_i) within 1–15 °C and long equilibrium time of 12 h.

Plateau values of ΔH_m vs. equilibrium time give 52 kJ/mol for 0.65 mM DDAB, obtained after 15 h. Neither the vesicle mean hydrodynamic diameter nor the zeta potential displays pronounced variation around T_m or CVC_2, indicating that there is no pronounced structural change in the bilayer structures.

Our findings stress that single DDAB Ves dispersions can be formed only in a very narrow range of concentrations (ca. 0.05–0.7 mM), and $T_m' \approx 9.5$°C value is reported here for the first time.

As DDAB dispersions have potential application in pharmaceutical industry, e.g., to prepare lipoplexes for cell transfection, the characterization of DDAB vesicles is demanded.

Acknowledgments

E.F. and R.D.A. thank FAPESP for grant, Grants 2011/03566-0 and 2011/07414-0, respectively. E.F. also thanks CNPq for Research Productivity Grant. The authors thank Professor Martin Malmsten for reading and commenting the text.

Appendix A. Supplementary data

Supplementary data associated with this article can be found, in the online version, at http://dx.doi.org/10.1016/j.colsurfa.2015.01.086.

References

[1] T. Kunitake, Y. Okahata, A totally synthetic bilayer membranes, J. Am. Chem. Soc. 99 (1977) 3360–3361.
[2] D. Li, G. Li, P. Li, L. Zhanga, Z. Liu, J. Wang, E. wanga, The enhancement of transfection efficiency of cationic liposomes by didodecyldimethylammonium bromide coated gold nanoparticles, Biomaterials 31 (2010) 1850–1857.
[3] E. Feitosa, Kinetic asymmetry in the gel–liquid crystalline state transitions of DDAB vesicles studied by differential scanning calorimetry, J. Colloid Interface Sci. 344 (2010) 70–74.
[4] M. Goto, S. Ishida, Y. Ito, N. Tamai, H. Matsuki, S. Kaneshina, Thermotropic and barotropic phase transitions of dialkyldimethylammonium bromide bilayer membranes: effect of chain length, Langmuir 27 (2011) 5824–5831.
[5] Y. Kondo, M. Abe, K. Ogino, H. Uchiyama, E.E. Tucker, J.F. Scamehorn, S.D. Christian, Stability of surfactant vesicles formed from cationic didodecyldimethylammonium bromide, Colloids Surf. B: Biointerfaces 1 (1993) 51–56.
[6] E.F. Marques, A. Khan, B. Lindman, A calorimetric study of the gel-to-liquid crystal transition in catanionic surfactant vesicles, Thermochim. Acta 394 (2002) 31–37.
[7] M.I. Viseu, K. Edwards, C.S. Campos, S.M.B. Costa, Spontaneous vesicles formed in aqueous mixtures of two cationic amphiphiles, Langmuir 16 (2000) 2105–2114.
[8] A. Caria, O. Regev, A. Khan, Surfactant–polymer interactions: phase diagram and fusion of vesicle in the didodecyldimethylammonium bromide–poly(ethylene oxide)–water system, J. Colloid Interface Sci. 200 (1998) 19–30.
[9] E.F. Marques, O. Regev, A. Khan, M.G. Miguel, B. Lindman, Vesicle formation and general phase behavior in the catanionic mixture SDS-DDAB-water. The Cationic-Rich Side, J. Phys. Chem. B 103 (1999) 8353–8363.
[10] T.F. Svitova, Y.P. Smirnova, S.A. Pisarev, N. Berezina, Self-assembly in double-tailed surfactants in dilute aqueous-solutions, Colloids Surf. A, Physicochem. Eng. Asp. 98 (1995) 107–115.
[11] F. Caboi, M. Monduzzi, Didodecyldimethylammonium bromide vesicles and lamellar liquid-crystal—a multinuclear nmr and optical microscopy study, Langmuir 12 (1996) 3548–3556.
[12] M. Dubois, T. Zemb, Phase behavior and scattering of double-chain surfactants in diluted aqueous solutions, Langmuir 7 (1991) 1352–1360.
[13] M.J. Blandamer, B. Briggs, P.M. Cullis, S.D. Kirby, J.B.F.N.J. Engberts, Reorganisation of alkyl chains in vesicles formed in aqueous solution by dialkyldimethylammonium bromide, $R_2N^+Me_2Br^-$ where $R = C_{12}H_{25}$, $C_{14}H_{29}$, $C_{16}H_{33}$ or $C_{18}H_{37}$, Chem. Soc. Faraday Trans. 93 (1997) 453–455.
[14] A. Lopes, K. Edwards, E. Feitosa, Extruded vesicles of dioctadecyldimethylammonium bromide and chloride investigated by light scattering and cryogenic transmission electron microscopy, J. Colloid Interface Sci. 322 (2008) 582–588.
[15] E. Feitosa, P.C.A. Barreleiro, G. Olofsson, Phase transition in dioctadecyldimethylammonium bromide and chloride vesicles prepared by different methods, Chem. Phys. Lipids 105 (2000) 201–213.
[16] Y. Ono, H. Kawasaki, M. Annaka, H. Maeda, Effects of micelle-to-vesicle transitions on the degree of counterion binding, J. Colloid Interface Sci. 287 (2005) 685–693.
[17] A. Fontana, P. De Maria, G. Siani, B.H. Robinson, Kinetics of breakdown of vesicles from didodecyldimethylammonium bromide induced by single chain surfactants and by osmotic stress in aqueous solution, Colloids Surf. B: Biointerfaces 32 (2003) 365–374.
[18] I. Grillo, J. Penfold, I. Tucker, F. Cousin, Spontaneous formation of nanovesicles in mixtures of nonionic and dialkyl chain cationic surfactants studied by surface tension and SANS, Langmuir 25 (2009) 3932–3943.
[19] J.F.A. Soltero, F. Bautista, E. Pecina, J.E. Puig, O. Manero, Z. Proverbio, P.C. Schulz, Rheological behavior in the didodecyldimethylammonium bromide/water system, Colloid Polymer Sci. 278 (2000) 37–47.
[20] H. Kawamura, M. Manabe, M. Myoujou, H. Katsuura, M. Shiomi, Partition coefficients of 1-alkanols between water and DDAB vesicle membrane determined by differential conductivity method, Oleo Sci. 58 (2009) 177–184.
[21] A. Caria, A. Khan, Phase behavior of catanionic surfactant mixtures: sodium bis(2-ethylhexyl)sulfosuccinate-didodecyldimethylammonium bromide-water system, Langmuir 12 (1996) 6282–6290.